Mechanical properties of individual microgel particles through the deswelling transition

Sara M. Hashmi*[a] and Eric R. Dufresne*[b]

Received 26th March 2009, Accepted 18th June 2009
First published as an Advance Article on the web 8th July 2009
DOI: 10.1039/b906051k

Microgels are important materials for both basic science and engineering and have wide applications from the study of phase transitions to the delivery of drugs. These micron and sub-micron particles, made of hydrogel materials, respond to solvent conditions. The most common microgels are environmentally sensitive, responding to temperature and pH. Our material of interest, poly (*N*-isopropylacrylamide) or NIPAM, undergoes a deswelling transition above a critical temperature. The deswelling behavior of this polymeric material has been thoroughly studied in ensemble microgel systems as well as in bulk hydrogel samples. We present measurements of the elastic properties of single microgel particles through the deswelling transition using atomic force microscopy. While the fully collapsed particle ($E = 123$ kPa) is ten times stiffer than a fully swollen one ($E = 13$ kPa), we observe a dramatic softening of the particle near the transition ($E = 3$ kPa).

1 Introduction

Over recent years, stimuli responsive materials have been developed which respond to changes in their solvent conditions. One of the most common type of stimuli-responsive materials is a class of materials called hydrogels—low density cross-linked polymer networks in water. For many hydrogels, the polymer network shrinks and swells with changes in temperature, pH, ionic strength, or solvent polarity.[1] Many hydrogels are biocompatible and have been used for scaffolding in tissue-engineering applications, topical drug-delivery applications, and even contact lenses.[2] In drug-delivery applications, the responsiveness of hydrogels allows for the controlled release of medication over time.[3–5] Hydrogels can be synthesized in bulk and in various other geometries including thin films and colloidal particles, called microgels.[6]

Thermoresponsive microgels undergo a phase transition once the solvent temperature reaches the lower critical solution temperature (LCST). The crosslinked network deswells as the temperature increases, and the particles collapse on themselves, segregating the polymer and expelling solvent. The amount of crosslinking in the material preparation has been shown to affect the swelling behavior.[7] In some systems this transition is quite sharp, and in others the transition is more gentle. The Flory–Rehner theory, which describes solvent–polymer interactions, has been used to describe the transition in particle size.[8]

The thermoresponsive properties of these materials make microgels an interesting tool for the study of fundamental questions such as those involving gelation, crystallization kinetics, and melting.[9,10] Members of the soft matter community especially have been tuning these materials through their phase transition by varying the temperature in order to investigate the effects of varying volume fractions within a single sample. In general, the interactions of microgel particles are soft,[11] but in some cases they are well-approximated as hard spheres.[9]

Material properties of individual colloidal particles affect bulk properties of suspensions and other material mixtures.[12,13] Measurements of individual microgels as they deswell may have important implications for both theory and experiments on bulk suspensions of microgels. As the characteristic length scale within the polymer network changes, so do the properties of the material. For example, the elastic modulus of a plasma-polymerized NIPAM thin film has been shown to increase by an order of magnitude, from approximately 200 kPa to 2 MPa, as the solvent temperature is increased from 298 to 310 K and the film thickness shrinks roughly 15%, from 73.7 nm to 63.7 nm.[14] Microgels similarly exhibit an order of magnitude increase in the modulus upon comparing their properties above the transition to those at room temperature.[15,16]

Characterization of such properties on the nano- or micro-scale is normally undertaken through deformation techniques such as nano-indentation using the sharp tip of an AFM or SEM probe.[17] AFM techniques have been used to study the morphology of both microgels and microgel monolayers.[18,19] However, techniques using sharp tips involve applying large, localized forces on a sample, often causing plastic deformation even in hard materials. For soft and biological materials, other techniques have been developed to minimize damage to the sample, such as manipulation with microneedles or microplates, and optical stretching.[20–23] Atomic force microscopy (AFM) techniques have also been modified to accommodate soft samples, through the attachment of large colloidal probes to AFM tips.[24]

In this report, we present AFM measurements of the modulus of individual microgel particles through the transition. Even though particle size decreases monotonically as the particle undergoes the deswelling transition, the measured modulus does

[a]*Department of Chemical Engineering, Yale University, 9 Hillhouse Avenue, New Haven, CT, 06510, USA. E-mail: sara.hashmi@yale.edu*
[b]*Departments of Mechanical & Chemical Engineering and Physics, Yale University, 9 Hillhouse Avenue, New Haven, CT, 06510, USA. E-mail: eric.dufresne@yale.edu*

not increase monotonically. We compare our results to theoretical predictions, and hope these results will provide insight into the behavior of individual microgels and motivation for further studies on materials made from microgels.

2 Materials and methods

2.1 Microgel particles

A 1% by weight colloidal suspension of deformable poly (*N*-isopropylacrylamide) (NIPAM) microgel particles was prepared by and obtained from Samia Laib. The particles were prepared by surfactant-free emulsion polymerization of *N*-isopropylacrylamide cross-linked with *N*,*N*′-methylenebisacrylamide; the details of the method have been fully described elsewhere by Routh and Vincent.[25]

2.2 Particle characterization

Phase analysis light scattering of the NIPAM microgels was performed (ZetaPALS, Brookhaven Instruments Corporation) to measure particle mobilities as a function of temperature *via* electrophoresis. At all temperatures the particles were found to have negative mobilities, with values ranging between -1.14 and -3.59×10^{-8} m^2 V^{-1} s^{-1}, comparable to published values for the mobility of NIPAM microgels.[26]

Particle size was characterized by dynamic light scattering (DLS) as a function of temperature, to capture the deswelling behavior that occurs close to 308 K (ZetaPALS, Brookhaven Instruments Corporation).

2.3 AFM substrate and sample preparation

Silicon wafers were cleaned by sonication in acetone and then methanol, followed by a deionized water (DIW) rinse. Residual organic material was cleaned off of the wafers by submersion in piranha etch (70% v/v sulfuric acid 98% with 30% v/v hydrogen peroxide, 30% aqueous) for approximately 45 minutes at 343 K. The wafers were then rinsed in DIW and dried on a 423 K hot plate.

The cleaned wafers were dip-coated with a layer of positively charged polymer, poly-L-lysine hydrobromide (PLL), M_w 30 000–70 000 (cas 25988-63-0, 047K5110, Sigma Life Science) to facilitate the immobilization of the negatively charged microgel particles on the surface.[27] Wafers were submerged in a solution of PLL, 10 mg mL^{-1}, in a filtered buffer solution of 10 mM HEPES (cas 7365-45-9, Sigma-Aldrich) with 100 mM NaCl, at pH 7 for two hours, and then rinsed in DIW and dried. Dried wafers were cut to size with a diamond scribe. The cut wafers were rinsed again, in DIW, and dried with N_2. The NIPAM microgel stock solution was diluted 5 times and 33 μL were deposited on the PLL-coated wafer. The samples were rinsed *in situ* in the AFM fluid sample holder to remove any non-adsorbed material. Microgels remain submerged in DIW for all measurements.

Sulfuric acid and hydrogen peroxide were obtained from T. J. Baker, and poly-L-lysine hydrobromide and HEPES from Sigma-Aldrich.

2.4 AFM tip preparation

A polystyrene particle was attached to an AFM cantilever to form the tip used to contact and investigate the microgels. A stock solution of 1μm diameter polystyrene spheres (Molecular Probes) was diluted to a concentration of approximately 100 particles per μL, and a few μL were deposited on a mica substrate. Tipless AFM cantilevers made of silicon nitride (NP-020, Veeco Probes) were dipped in optical glue (Norland) placed on the same mica substrate, and then touched to the polystyrene particles to attach them to the cantilever. Viewing the cantilever through an optical zoom lens attached to the AFM provided verification that the particle was attached to the end of the cantilever. The optical glue was then cured under ultraviolet light for 10–15 minutes. The force constant of the cantilever beams with polystyrene particles attached was measured using force contact mode against a calibrated cantilever beam (FCL-5, Nanoscience Instruments).

2.5 AFM measurements and analysis

Force-deformation data of the polystyrene probe contacting the microgels in aqueous solution was obtained in Contact Mode using an atomic force microscope from Veeco (Nanoscope 2). Microgel particles were viewed and then centered in the field of view before the force mode was engaged. After the force measurements were taken, the sample was viewed again to confirm that the particle position had not drifted during measurement. The temperature of the AFM was controlled using a specialized Air–Fluid Heater Package for Multimode SPMs (MMHC-A60, Veeco Metrology). Data was gathered on a single particle as it underwent the phase transition, with force measurements obtained at six temperatures between 300 K and 313 K, with a roughly 2 K increment between measurements. Several images were obtained at those temperatures to illustrate the particle morphology through the transition. Measurements were also obtained on ensembles of particles both below and above the transition, at 300 K and 313 K.

When the AFM was engaged in force mode, the stage was in constant motion with the AFM tip probing the particle at a controllable rate. To avoid viscous contributions to the force measurements, we measured the modulus of a particle at room temperature at frequencies between 0.05 and 7 Hz. Even with a variation of two orders of magnitude in frequency, the modulus results varied by only 10%. Subsequent force measurements were gathered at a frequency of 1 Hz, to fall safely within the regime where the microgel particles remain in equilibrium.

3 Results and discussion

3.1 Particle size results

The morphology of microgels at room temperature and through the deswelling transition was captured with an AFM in contact mode. Sample images of the NIPAM microgel particles at room temperature are shown in Fig. 1(a). The particles appear to be slightly elongated in the direction of the raster scan of the cantilever. Images of the same particle at different temperatures exhibit monotonic dependence of the size on temperature, as shown in Fig. 1(b). The particle size seems to remain relatively

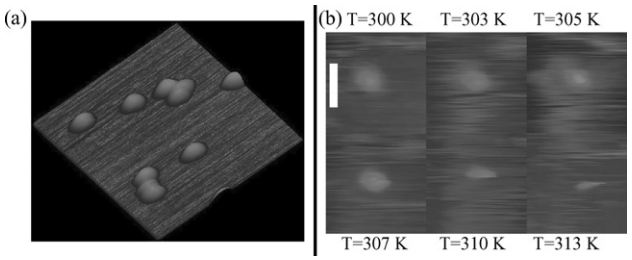

Fig. 1 AFM images of microgel particle morphology: (a) a set of particles viewed at an angle from the top, at room temperature. The image is 10 μm on each side. (b) A series of images of a single particle at different temperatures through the deswelling phase transition. The scale bar represents 2 μm.

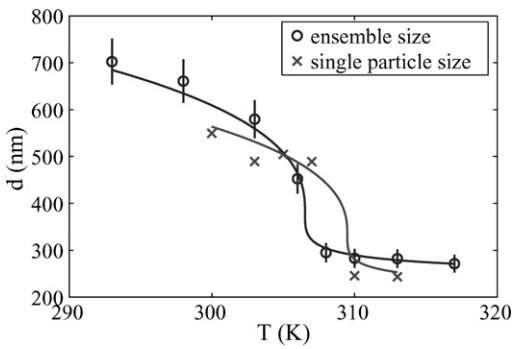

Fig. 2 Particle size as a function of temperature. The circles represent an ensemble measurement of particle size with DLS, while the ×'s show size measurements of a single-particle with AFM. The solid line through each measurement denotes a prediction of the Flory–Rehner theory.

constant until about 310 K, when it shrinks to approximately half its size at room temperature.

We quantify the deswelling of the particles by DLS. The ensemble particle size measurements were obtained as a function of temperature, as shown with circles in Fig. 2. The polydispersity in the ensemble was approximately 7% at all temperatures, as shown by the error bars. At room temperature the particles were approximately 700 nm in size, and shrunk to a size below 300 nm well above room temperature. The transition was fairly smooth, and the transition temperature seemed to be near 307 K. The size of a single particle through the transition was estimated from the series of AFM images shown in Fig. 1(b). Particle size d was obtained with $d = (6V/\pi)^{1/3}$, and particle volume V estimated from the AFM images using $V = HL^2$, where H is the height of the particle and L is a measure of its in-plane dimension. The particle size estimates through AFM are shown with ×'s in Fig. 2. The transition temperature of this single particle seems to be near 310 K, a few degrees higher than the ensemble measurement.

3.2 Model for the temperature dependence of particle size

Flory–Rehner theory makes predictions which capture the swelling behavior of bulk gels in equilibrium. Swelling equilibrium at each temperature T corresponds to the condition when the osmotic pressure, Π, is zero:

$$\Pi = \frac{k_B T}{\alpha^3}\left(-\phi - \ln(1-\phi) - \chi\phi^2 + \frac{\phi_0}{N_{gel}}\left[\left(\frac{\phi}{2\phi_0}\right) - \left(\frac{\phi}{\phi_0}\right)^{1/3}\right]\right) \quad (1)$$

where k_B is the Boltzmann constant, ϕ the volume fraction of polymer within the particle, ϕ_0 the volume fraction in the collapsed state, χ the Flory solvency parameter, α the monomer size, and N_{gel} the average number of monomers between cross-links.[8,28] The first two terms of eqn (1) are the entropy of mixing polymer with solvent, the third term is the enthalpy of mixing and the fourth and final term is the contribution to the osmotic pressure from the connectivity of the network.[29,30] The Flory solvency parameter describes the transition, $\chi(T, \phi) = \chi_1(T) + \chi_2\phi + O(\phi^2) + \ldots$; χ depends upon temperature and has been shown empirically to also depend upon polymer volume fraction.[31,8] The temperature-dependent part of χ is given by the Flory–Rehner theory:

$$\chi_1 = \frac{\Delta F}{k_B T} = \frac{1}{2} - A\left(1 - \frac{\Theta}{T}\right) \quad (2)$$

where $\Theta = 2\Delta H/(2\Delta S + k_B)$ is known as the Θ temperature. The parameter $A = (2\Delta S + k_B)/k_B$, where ΔS and ΔH are the changes in entropy and enthalpy, respectively, per monomer for the deswelling transition. The Θ temperature refers to the temperature where excluded volume effects within the polymer network vanish, and is slightly above the critical temperature of the phase transition.[32]

To generate the Flory–Rehner prediction for the dependence of particle size on temperature, we first set $\Pi = 0$ using eqn (1) to solve for the volume fraction ϕ as a function of temperature. For isotropic swelling, particle size is inversely related to volume fraction:

$$\frac{\phi}{\phi_0} = \left(\frac{d_0}{d}\right)^3 \quad (3)$$

where d is the particle diameter and d_0 and ϕ_0 are the diameter and polymer volume fraction in the collapsed state above the transition temperature. Following the method of Fernandez–Barbero *et al*, we first considered that χ_1 falls in the range $0 < \chi_1 < 1$ for NIPAM microgels.[8] We also considered that the Θ temperature typically sits above the observed transition temperature, and that in microgels $\phi_0 < 1$.[6,8] We generated a Flory–Rehner solution using the following set of parameters: $\phi_0 = 0.7$, $\Theta = 310$ K, $N_{gel} = 300$, $A = -7$, $\chi_2 = 0.65$, and $d_0 = 278$ nm, as obtained from the ensemble measurements. We compared this solution to the ensemble measurements, as seen with the solid line through the circles in Fig. 2. The Θ temperature sat above the transition temperature for the particles, which seems to be near 307 K, judging by the sizing data. The fit of $\phi_0 < 1$ suggested that the microgel particles still contain 30% solvent within them even well above the transition temperature. This result of solvent within a deswollen microgel has also been seen in other studies of NIPAM microgel particles.[8] To generate a prediction for the single particle size measurements we used the same set of parameters as the ensemble measurement, with the exception that the transition temperature was shifted

higher to $\Theta = 313$ K, and $d_0 = 243$ nm for the single particle size measurements. These adjustments reflect the slightly higher transition temperature and smaller collapsed particle size for the single particle, as seen with the line through the ×'s in Fig. 2. Parameters A and Θ yielded values for the entropic and enthalpic changes of $\Delta S = -4.5\ k_B$ and $\Delta H = -4.1\ k_B T$ per molecule. These values are consistent with the behavior of the NIPAM microgels, as negative enthalpic and entropic changes signify that the transition occured at a lower critical temperature (LCST).[8,28,33]

3.3 Particle modulus results

As deswelling occurs we expect the mechanical properties of the particles to change along with their size. To characterize this change we used the AFM to measure force *versus* deformation curves on particles below and above the transition temperature. The raw data is conveniently represented by plotting the force *versus* deformation behavior on a log–log plot, as shown in the left-hand plots of Fig. 3. At small deformations, the force measurement is limited by the force resolution of the AFM, of the order of 10^{-11} N. At the lowest resolvable deformations, the force depends on the deformation through a power law of 3/2, as denoted by the line with slope 3/2 superimposed on the raw data. At more pronounced deformations the slope of the force curve greatly increases, and in some data sets appears to diverge. In measurements taken above the transition temperature, this deviation from the 3/2 power law occurs more abruptly than in measurements below the transition, as can be seen in the left-hand plots of Fig. 3. Given the force-deformation measurements on these particles, we calculated that thermal fluctuations alone would compress a particle less than 2% of its radius both below and above the transition, suggesting that it is indeed reasonable to treat microgels with comparable crosslinking densities as hard spheres.

The power-law region of the plot suggests elastic Hertzian contact between the microgel sample and the colloidal probe on the cantilever tip. The force F required to indent an elastic sphere in the Hertzian model varies as a power law with the deformation h:

$$F = \frac{4}{3}\frac{(a_{red})^{1/2}}{(1-\nu^2)}Eh^{3/2} \quad (4)$$

where E is the elastic (Young's) modulus, ν is the Poisson ratio and a_{red} is the reduced radius

$$a_{red} = \frac{1}{\frac{1}{a} + \frac{1}{a_{cp}}} \quad (5)$$

which depends on both a, the radius of the microgel particle and a_{cp}, the radius of the colloidal probe particle. We assume $\nu = 0.36$. Given the force *versus* deformation curve for the particles, the modulus *versus* deformation curve ωas measured by inverting eqn (4) to determine the modulus.[34,35] For elastic materials, the Hertzian model predicts a constant modulus for small sample deformations. In macroscopic hydrogel films of NIPAM, the power law region of the force–deformation curves was shown to persist until almost 20% strain.[14]

For the modulus of the microgel particles to be appropriately described by the Hertz model, we expect that the modulus should remain constant for small h. Investigating representative force–deformation plots below and above the transition, we see that the modulus reaches a plateau at small deformations; this value gives the measurement of the modulus. The modulus was approximately 6 times larger at 313 than at 300 K, as shown in the right-hand plots in Fig. 3. These values are 82 kPa and 13 kPa, respectively. Near room temperature the modulus remained relatively constant up to approximately 100 nm as compared to 50 nm at 313 K. The model broke down much more abruptly for the particle above the transition temperature. The Hertzian fit seemed to hold fairly well up until $h/d \approx 0.17$ for both temperatures, as shown by the arrows in Fig. 3. The measured values of the modulus at small deformation can be used to fit the force–deformation curves using eqn (4), as shown by the solid straight lines in the left-hand plots of Fig. 3.

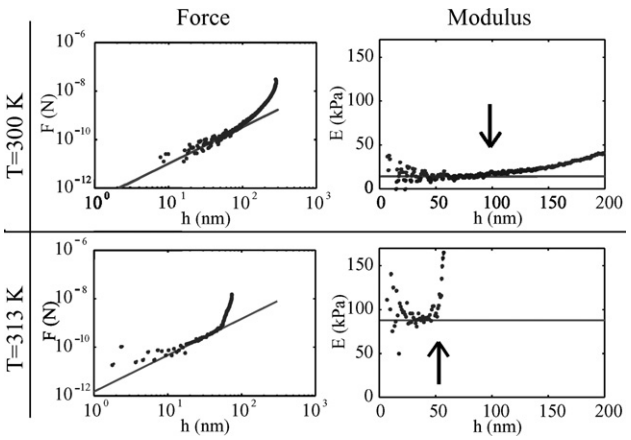

Fig. 3 Force and apparent modulus *versus* deformation: the top row of data was obtained on a particle at 300 K, and the bottom row on a different particle at 313 K. The Young's modulus is used to fit both plots at each temperature; below the transition the modulus is 13 kPa and above 82 kPa. The arrows indicate $h/d \approx 0.17$ at each temperature.

The measurements taken below and above the transition differed by almost an order of magnitude, suggesting that the increase in temperature caused an increase in the modulus. We repeated the measurements described above on a collection of particles both below and above the transition temperature. The average value of the modulus measured on nine microgel particles at 300 K was 8 ± 1.4 kPa, and the average modulus of six particles at 313 K was 86 ± 22 kPa. This gave a ten-fold increase in the modulus over a 13 K increase in the temperature, comparable to reported values.[15,16] However, the distribution of moduli of particles at the same temperature suggested that inter-particle variation of properties such as size and crosslinking also played a role. Isolating the effect of the deswelling on the modulus therefore requires measurements on a single particle through the transition.

Single particle force–deformation measurements through the transition revealed an intriguing softening which could not be captured by simply measuring below and above the transition. The modulus began to increase with temperature, then decreased below and through the transition, and then increased more sharply afterward, as shown in Fig. 4. The modulus decreased by almost an order of magnitude, a factor of ~7, between the

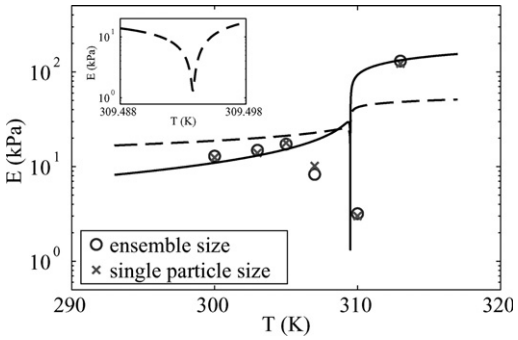

Fig. 4 Single particle modulus as a function of temperature: open circles show the modulus extracted with the ensemble particle size, while the ×'s denote the modulus extracted with the single particle measurement of size. The dashed and solid lines denote fits to theory, as discussed in the text. The inset shows a region of 0.01 K around the transition temperature of the dashed line fit.

temperatures of 305 and 310 K, and then grew by a factor of 40 from 310 to 313 K.

Since the Hertzian model requires an input of particle size, we used both measures of particle size to confirm the robustness of the softening. The modulus extracted from the raw data using ensemble measurement of size are shown with open circles in Fig. 4. The modulus values extracted using particle size as measured from the single particle AFM measurements are shown with ×'s in Fig. 4. The modulus measurements were not extremely sensitive to variations in particle size: though the estimated single particle size differs from the ensemble, as seen in Fig. 2, the use of either size to extract the modulus yielded similar results.

3.4 Model for the temperature dependence of particle modulus

The same Flory–Rehner theory which was applied to the particle size measurements can also be used to account for the softening observed in the transition region for bulk gels.[28] The Young's modulus is a combination of the bulk and shear moduli:

$$E = \frac{9K\mu}{3K + \mu} \tag{6}$$

The bulk modulus K is the inverse of the isothermal compressibility:

$$K = \phi \frac{\delta \Pi}{\delta \phi}|_T \tag{7}$$

where Π is the osmotic pressure.[36] Given the Flory–Rehner formulation of the osmotic pressure given in eqn (1) the bulk modulus is given by:

$$K = \frac{k_B T}{\alpha^3}\left[\frac{\phi^2}{1-\phi} - 2\chi_1\phi^2 - 3\chi_2\phi^3 + \frac{\phi_0}{N_{gel}}\left(\frac{\phi}{2\phi_0} - \frac{1}{3}\left(\frac{\phi}{\phi_0}\right)^{1/3}\right)\right] \tag{8}$$

The Flory shear modulus, for polymer networks in solvent, is given by:

$$\mu = \left(\frac{\phi_0 k_B T}{2N_{gel}\alpha^3}\right)\left(\frac{\phi}{\phi_0}\right)^{1/3} \tag{9}$$

and scales inversely with the radius of the particle.[36,37] The Flory–Rehner theory predicts that the shear modulus monotonically increases with temperature for networks which deswell upon crossing an LCST, while the bulk modulus may show non-monotonic behavior through a phase transition.[28,29] For transitions which go through the critical point, Flory–Rehner theory predicts a bulk modulus which vanishes to 0.[36] Given the Flory–Rehner predictions for the bulk and shear moduli, the Poisson ratio ($\nu = (3K - 2\nu)/2(3K + \nu)$) may also be expected to change non-monotonically through the transition.

The parameters used in the Flory–Rehner prediction for particle size can also be used to fit the modulus measurements through the transition, with the addition of the parameter α, the monomer size, which falls out of the prediction for ϕ when $\Pi = 0$ in eqn (1). Note that α sets the scale of the modulus but not its temperature dependence. We chose $\alpha = 6.7 \times 10^{-10}$ m, consistent with the range of values found in the literature for NIPAM microgels.[8,38] We compared the Flory–Rehner theory to the data obtained across the transition, as seen with the dashed line in Fig. 4. The Flory–Rehner theory developed for bulk gels qualitatively captured softening at the transition and stiffening above. However, even with adjustments to the parameters used to match the microgel sizing data, the Flory–Rehner theory predicts a sharp transition occurring over a small range of temperatures, as shown in the inset of Fig. 4. Furthermore, the Flory–Rehner theory predicts that the modulus will increase across the transition by a factor of 2 or 3 only, due to the scaling of the Flory shear modulus. Adjusting the parameters does not account for the order of magnitude increase in the measurements from below to above the transition. Using the predicted temperature dependence for the Poisson's ratio instead of an averaged value also preserves the features of the curve: $0.31 < |\nu| < 0.49$, giving a less than 4% difference in the Young's modulus at all temperatures except 313 K, where the difference is 13%. Interestingly, the predicted Poisson's ratio behaves non-monotonically: $\nu < 0$ near the transition temperature, suggesting that the system may be close to the critical point of the phase transition.[36]

The order of magnitude increase in the measurements from below to above the transition suggests that the Young's modulus may scale inversely with particle volume rather than particle size. While the Flory shear modulus varies inversely with particle radius, rubber elasticity theory gives a prediction which scales inversely with particle volume:

$$\mu = \left(\frac{k_B T}{2N_{gel}\alpha^3}\right)\phi \tag{10}$$

which is useful for describing cross-linked polymer networks in the absence of solvent.[39] Interestingly, when combined with the Flory–Rehner prediction for the bulk modulus, the inverse volume scaling of rubber shear elasticity does indeed capture the order of magnitude jump in the Young's modulus from below to well above the transition, as seen by comparing the two fits in Fig. 4.

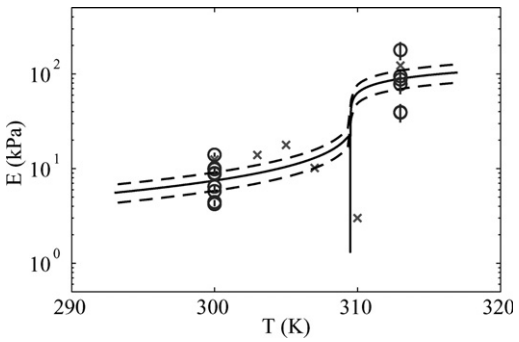

Fig. 5 Particle-to-particle variation of modulus: the circles represent the measurements taken on the ensembles of particles both below and above the phase transition. Nine particles are measured at 300 K, and six at 313 K. The ×'s are the single particle data from Fig. 4. The solid line is a fit to the average below and above the transition, and the dashed lines represent the expected spread due to polydispersity.

We compared the prediction of the Young's modulus using the Flory bulk modulus along with the rubber elasticity shear modulus to the multiple particle measurements as well, shown by the solid line in Fig. 5. The prediction has been shifted to capture the average of the measurements both below and above the transition, by using the deswollen particle size from the ensemble DLS measurements. The spread in the prediction due to the polydispersity in the ensemble sizes is shown with the dashed lines above and below the solid line: the scatter in the measurements above and below the transition are comparable, but outside the spread of the prediction. Note that the measurements on the single particle shown with the ×'s fall within the scatter of the measurements both below and above the transition, but outside the spread due to polydispersity. This signifies that particle size variation is not the only factor leading to differences in modulus measurements between particles. Other characteristics may play an important role as well, such as the heterogeneous nature of the crosslinking.[8]

4 Conclusion

The characterization of the microgel particles through the deswelling transition revealed a monotonic dependence of particle size with temperature. However, modulus measurements taken on an AFM reveal non-monotonic behavior, exhibiting a softening through the transition and then a stiffening above the transition. Swollen particles at room temperature had Young's moduli on average 8 KPa. At temperatures well above the phase transition, the particles stiffened by an order of magnitude to an average 86 KPa in the collapsed state. The monotonic decrease in the size of the polymer network from low to high temperatures can qualitatively account for the overall stiffening as the material transitions from the swollen to the collapsed state. Through the transition itself, the Young's modulus of the particles softened due to a softening of the bulk modulus of the material, while the shear modulus increased monotonically.

The well-known Flory–Rehner theory for bulk gels captures the deswelling behavior of the microgel particles, both in the ensemble and for single particle measurements. However, when used to describe the mechanical properties of the particles through the transition, Flory–Rehner theory captures only the basic qualitative features of the transition for microgels. The theory does not account for the breadth of the transition, and does not explain the order of magnitude increase of stiffness between the swollen and collapsed states. Our observations suggest that the modulus of the microgel particle may scale inversely with particle volume rather than radius. Substituting the shear modulus from rubber elasticity theory captures this order of magnitude increase. Furthermore, the inverse volume dependence of rubber shear elasticity also begins to explain the scatter seen in the modulus data taken on several particles both below and above the transition. The scatter in the data also suggests that more than simply polydispersity may be required to fully account for the difference in modulus between particles: variations in crosslinking between particles may also play a role.

The heterogeneous nature of the crosslinking within the microgels may help to explain the broadening of the transition seen in the measurements. The breadth of this transition is not accounted for by the Flory–Rehner theory, which assumes homogenous crosslinking conditions throughout the gel. Microgel particles, however, are prepared by a process in which polymerization and crosslinking occur in the same step,[40,41] leading to a higher concentration of crosslinking in the core of the particle.[8] This heterogeneity in crosslinking density may lead to spatial variation in the transition temperature throughout the particle, thereby broadening the transition.[42] Furthermore, phase transitions are well known to broaden due to finite size effects, which may also play a role in these microgel systems.[43,44]

The effects shown here should depend on particle preparation and the details of the chemical recipe used to make the microgel particles. A more complete characterization of the modulus behavior in a variety of crosslinking environments would help to further elucidate the effects of heterogeneity and finite size. Very loosely crosslinked microgels may provide a unique material to investigate the effect of single particle material properties on the properties of bulk suspensions. Independent or simultaneous measurements of a second material parameter could provide more insight into the compressibility of microgels and appropriate modifications to the theory for bulk gels. In principle, AFM measurements may also be able to measure torque, thereby providing measurement of the shear modulus of these particles as a function of temperature to investigate the scaling behavior. Furthermore, the present findings suggest that microgels may also provide a novel platform for the study of finite-size effects in phase transitions.

Acknowledgements

The authors gratefully acknowledge helpful conversations with Alberto Fernandez-Nieves. The authors wish to thank Menachem Elimelech for providing the AFM and ZetaPALS facilities at Yale University, Samia Laib and Alex Routh of the University of Cambridge for synthesizing and providing the NIPAM microgel particles, and Dean Schmidt and Pat McPhail from Veeco Instruments for their assistance with the AFM heater.

References

1 B. R. Saunders, H. M. Crowther, G. E. Morris, S. J. Mears, T. Cosgrove and B. Vincent, *Colloids Surf., A*, 1999, **149**, 57.
2 P. C. Nicolson and J. Vogt, *Biomaterials*, 2001, **22**, 3273.

3 Y. Qiu and K. Park, *Adv. Drug Delivery Rev.*, 2001, **53**, 321.
4 D. T. Eddington and D. J. Beebe, *Adv. Drug Delivery Rev.*, 2004, **56**, 199.
5 V. Nerapusri, J. L. Keddie, B. Vincent and I. A. Bushnak, *Langmuir*, 2007, **23**, 9572.
6 R. Pelton, *Adv. Colloid Interface Sci.*, 2000, **85**, 1.
7 K. Kratz, T. Hellweg and W. Eimer, *Polymer*, 2001, **42**, 6631.
8 A. Fernández-Barbero, A. Fernández-Nieves, I. Grillo and E. López-Cabarcos, *Phys. Rev. E: Stat., Nonlinear, Soft Matter Phys.*, 2002, **66**, 051803.
9 A. M. Alsayed, M. F. Islam, J. Zhang, P. J. Collings and A. G. Yodh, *Science*, 2005, **309**, 1207.
10 J. Wu and Z. Hu in *Dekker Encyclopedia of Nanoscience and Nanotechnology*, ed. J. A. Schwarz, C. I. Contescu and K. Putyera, Taylor and Francis, London, 2004.
11 M. Stieger, J. S. Pedersen, P. Lindner and W. Richtering, *Langmuir*, 2004, **20**, 7283.
12 H. Senff and W. Richtering, *Colloid Polym. Sci.*, 2000, **278**, 830.
13 S. Adams, W. J. Frith and J. R. Stokes, *J. Rheol.*, 2004, **48**, 1195.
14 X. Cheng, H. E. Canavan, M. J. Stein, J. R. Hull, S. J. Kweskin, M. S. Wagner, G. A. Somorjai, D. G. Castner and B. D. Ratner, *Langmuir*, 2005, **21**, 7833.
15 O. Tagit, N. Tomczak and G. J. Vancso, *Small*, 2008, **4**, 119.
16 J. Wiedemair, M. J. Serpe, J. Kim, J.-F. Masson, L. A. Lyon, B. Mizaikoff and C. Kranz, *Langmuir*, 2007, **23**, 130.
17 W. C. Oliver and G. M. Pharr, *J. Mater. Res.*, 2004, **19**, 3.
18 S. Höfl, L. Zitzler, T. Hellweg, S. Herminghaus and F. Mugele, *Polymer*, 2007, **48**, 245.
19 P. A. FitzGerald, D. Dupin, S. P. Armes and E. J. Wanless, *Soft Matter*, 2007, **3**, 580.
20 S. Felder and E. L. Elson, *J. Cell Biol.*, 1990, **111**, 2513.
21 M. Radmacher, M. Fritz, C. M. Kacher, J. P. Cleveland and P. K. Hansma, *Biophys. J.*, 1996, **70**, 556.
22 O. Thoumine and A. Ott, *J. Cell Sci.*, 1997, **110**, 2109.
23 J. Guck, R. Ananthakrishnan, H. Mahmood, T. J. Moon, C. C. Cunningham and J. Käs, *Biophys. J.*, 2001, **81**, 767.
24 H.-J. Butt, B. Cappella and M. Kappl, *Surf. Sci. Rep.*, 2005, **59**, 1.
25 A. F. Routh and B. Vincent, *Langmuir*, 2002, **18**(14), 5366.
26 M. J. García-Salinas, M. S. Romero-Cano and F. J. de las Nieves, *J. Colloid Interface Sci.*, 2001, **241**, 280.
27 R. Wittmer, J. A. Phelps, W. M. Saltzman and P. R. V. Tassel, *Biomaterials*, 2007, **28**, 851.
28 S. Hirotsu, *Phase Transitions*, 1994, **47**(3), 183.
29 T. Tanaka, S. Ishiwata and C. Ishimoto, *Phys. Rev. Lett.*, 1977, **38**, 771.
30 T. Tanaka, *Phys. Rev. Lett.*, 1978, **40**, 820.
31 B. E. Eichinger and P. J. Flory, *Trans. Faraday Soc.*, 1968, **64**, 2035.
32 M. Doi and S. F. Edwards, *The theory of polymer dynamics*, Oxford University Press, New York, 1986.
33 T. Somcynsky, *Polym. Eng. Sci.*, 1982, **22**, 58.
34 E. K. Dimitriadis, F. Horkay, J. Maresca, B. Kachar and R. S. Chadwick, *Biophys. J.*, 2002, **82**, 2798.
35 L. D. Landau and E. M. Lifshitz, *Theory of Elasticity*, Butterworth-Heinemann, Oxford, 3rd edn, 1986.
36 S. Hirotsu, *J. Chem. Phys.*, 1991, **94**, 3949.
37 P. J. Flory, *Principles of polymer chemistry*, Cornell University Press, New York, 1966.
38 K. Kubota, S. Fujishige and I. Ando, *Polym. J.*, 1990, **22**, 15.
39 L. R. G. Treloar, *The physics of rubber elasticity*, Oxford University Press, 2005.
40 A. Guillermo, J. P. C. Addad, J. P. Bazile, D. Duracher, A. Elaissari and C. Pichot, *J. Polym. Sci., Part B: Polym. Phys.*, 2000, **38**, 889.
41 X. Wu, R. H. Pelton, A. E. Hamielec, D. R. Woods and W. McPhee, *Colloid Polym. Sci.*, 1994, **272**, 467.
42 C. Wu and S. Zhou, *Macromolecules*, 1997, **30**, 574.
43 T. Kajander, A. L. Cortajarena, E. R. G. Main, S. G. J. Mochrie and L. Regan, *J. Am. Chem. Soc.*, 2005, **127**, 10188.
44 Y. Imry, *Phys. Rev. B: Condens. Matter Mater. Phys.*, 1980, **21**(5), 2042.

